Electronic Supplementary Material (ESI) for ChemComm.

Ammonium ion-promoted electrochemical production of synthetic gas from water and carbon dioxide on fluorine-doped tin oxide electrode

Shin-ichi Naya,[a] Hisayoshi Yoshioka,[b] and Hiroaki Tada[b] *

[a] *Environmental Research Laboratory, Kindai University, 3-4-1, Kowakae, Higashi-Osaka, Osaka 577-8502, Japan.*

[b] *Graduate School of Science and Engineering, Kindai University, 3-4-1, Kowakae, Higashi-Osaka, Osaka 577-8502, Japan*

*Author to whom correspondence should be addressed.

Professor Hiroaki Tada

Tel: +81-6-6721-2332; Fax: +81-6-6727-2024

E-mail: h-tada@apch.kidai.ac.jp

Experimental

Electrochemical measurements and characterization

Fluorine-doped tin(IV) oxide film coated on glass (FTO, Aldrich TEC7, sheet registance = 7 Ω) was used as the working electrode. For the linear sweep voltammogram (LSV) measurements, a three-electrode cell was fabricated with a structure of glassy carbon | 0.1 M Na_2SO_4 and/or 0.1 M $NaHCO_3$ | FTO, Ag/AgCl. Before the measurement, Ar or CO_2 gas was bubbled into the electrolyte solution for 30 min. The LSVs were collected by using a galvanostat/potentiostat (HZ-7000, Hokuto Denko). X-ray diffraction (XRD) patterns were collected by means of a Rigaku SmartLab X-ray diffractometer operating at 40 kV and 100 mA. Scanning electron microscopy (SEM) images were taken by Hitachi SU8230 at an applied voltage of 20 kV. X-ray photoelectron spectroscopic (XPS) measurements were carried out by a Kratos Axis Nova X-ray photoelectron spectrometer using a monochromated Al Kα as X-ray source with 15 kV and 10 mA. The energy reference is C1s (284.6 eV).

Electrochemical CO_2 reduction reaction

A two compotent three-electrode cell was fabricated with a structure of glassy carbon | 0.1 M $(NH_4)HCO_3$ aq. (pH 6.7) | Nafion | 0.1 M $(NH_4)HCO_3$ aq. (pH 6.7) | FTO, Ag/AgCl. Before the measurement, CO_2 gas was bubbled into the electrolyte solution in each component for 30 min. Chronoamperometry curves were obtained under CO_2 flow with a constant rate of 100 mL min^{-1} by using a galvanostat/potentiostat (HSV-110, Hokuto Denko). The potential of FTO electrode was maintained at -1.3 V vs. SHE. The gaseous products were quantified by gas chromatography (GC-2010Plus with BID-detector, Shimadzu, column = Rt-Mseive 5A, Shimadzu GLC, He flow rate = 10 mL min^{-1}). The products in the electrolyte solution were quantified by NMR (JNM-AL400, JEOL Resonance). D_2O and dimethylsulfoxide were used for the signal lock and internal standard, respectively.

NH_4^+ ion adsorption

FTO nanopartiles were prepared by the reported procedure.[S1] Adsorption isotherm of NH_4^+ ions was obtained by exposing FTO nanoparticles (100 mg) to aqueus solutions with different concentrations of $(NH_4)HCO_3$ at 25°C for 3 h in the dark. The resulting FTO nanoparticles adsorbed NH_4^+ ions were collected by centrifugation and dried in vacuo. After removing particles from supernatante by using membrane filter, the remaining NH_4^+ ions were quantified by the indophenol blue method. Difuse reflectance infrra red Foulier transform spectroscopy (DRIFT) was measured by means of FTIR-8400S spectrometer (Shimadzu) with the diffuse reflectance unit (DRS-8000, Shimadzu). ζ -Potential measurements were carried out using a Zetasizer Nano ZS (Malvern

Instruments). Samples were prepared by dispersing FTO (15 mg) into an aqueous solution (100 mL) of $(NH_4)_2SO_4$ (0−20 mM), and ultrasonicated for 30 min. The samples were introduced to a disposable folded capillary cell (DTS1060). Electrophoretic mobilities were measured at 25 °C using the Malvern M3-PALS, and converted to ζ-potential by the Henry's equation.

Reference

S1. H. Xu, L. Shi, Z. Wang, J. Liu, J. Zhu, Y. Zhao, M. Zhang, S. Yuan, *ACS Appl. Mater. Interfaces*, 2015, **7**, 27486-27493.

Table S1 Electrocatalytic activity of the catalysts for electrochemical production of synthetic gas

Electrocatalyst	Current density	Faradaic efficiency		CO/H_2 molar ration	Electrolyte	Applied bias	Reference
	$mA\ cm^{-2}$	CO	H_2				
Sn/FTO	2.4	30	55	0.55	0.1 M $(NH_4)HCO_3$	0.9 V vs RHE	This work
Ni/AGF	10	50	50	1.00	0.5 M $KHCO_3$	0.6 V vs RHE	Ref. S2
Ag	80	33	66	0.50	0.5 M $KHCO_3$	1.8 V vs SCE	Ref. S3
$[Mn(bpy)(CO)_3Br]$	0.3	22	47	0.47	phosphate buffer	1.4 V vs Ag/AgCl	Ref. S4
Ru complex	1.5	30	70	0.43	0.5 M NaHCO3	1.5 V vs RHE	Ref. S5
Ru complex	0.8	65	30	2.17	0.5 M NaHCO3	1.2 V vs RHE	Ref. S5
Metal-Doped Nitrogenated Carbon	30	10	90	0.11	0.5 M $KHCO_3$	0.9 V vs RHE	Ref. S6
Ag	3	83	12	6.92	0.1 M $KHCO_3$	1.0 V vs RHE	Ref. S7
Ag/C	32	70	30	2.33	0.5 M $KHCO_3$	1.5 V vs Ag/AgCl	Ref. S8
$Cu@SnO_2$	22	90	5	18.00	0.5 M $KHCO_3$	0.9 V vs RHE	Ref. S9
Pd/C	0.3	40	50	0.80	0.5 M $KHCO_3$	0.6 V vs RHE	Ref. S10
Au film	30	-	-	14.00	0.5 M $KHCO_3$	0.65 V vs RHE	Ref. S11
Cu on Au film	20	-	-	0.66	0.5 M $KHCO_3$	0.65 V vs RHE	Ref. S11
Cu-In	0.8	32	30	1.07	0.1 M $KHCO_3$	0.9 V vs RHE	Ref. S12
Co_3O_4-CDots-C_3N_4	1	90	10	9.00	0.5 M $KHCO_3$	0.6 V vs RHE	Ref. S13
Au/Titanate	45	70	30	2.33	0.5 M $KHCO_3$	0.9 V vs RHE	Ref. S14
Zn	12	25	60	0.42	0.1 M $KHCO_3$	0.9 V vs RHE	Ref. S15
porous Sn	-	30	60	0.50	0.1 M $NaHCO_3$	0.6 V vs RHE	Ref. S16
AgP_2	13	38	62	0.61	0.5 M $KHCO_3$	0.6 V vs RHE	Ref. S17
0.1 %BDD	-	29	42	0.69	0.1 M $KClO_4$	2.1 V vs Ag/AgCl	Ref. S18
0.1 %BDD	-	2.6	15	0.17	0.1 MKCl	2.1 V vs Ag/AgCl	Ref. S18
Sn	-	3.4	3.9	0.87	0.1 M $KClO_4$	2.0 V vs Ag/AgCl	Ref. S18
Sn	-	2.6	5.4	0.48	0.1 M KCl	2.0 V vs Ag/AgCl	Ref. S18
$Zn_xCd_{1-x}S$-Amine	25	60	40	1.50	0.5 M $NaHCO_3$	1.16 V vs RHE	Ref. S19
Ag-SnS_2	38.8	20.5	19.5	1.05	0.5 M $KHCO_3$	1.0 V vs RHE	Ref. S20
Au	0.36	52	48	1.08	0.25 M $KHCO_3$	0.8 V vs RHE	Ref. S21
Co single atom-graphite-Co nanoparticle	10	45	50	0.90	0.1 M $KHCO_3$	0.8 V vs RHE	Ref. S22
ZnO (Lattice Perfect)	22	22	65	0.34	0.1 M $KHCO_3$	1.4 V vs RHE	Ref. S23
ZnO (Lattice distorted)	25	65	32	2.03	0.1 M $KHCO_3$	1.4 V vs RHE	Ref. S23
CoNi-NC	50	55	43	1.28	0.5 M $KHCO_3$	0.9 V vs RHE	Ref. S24
Pd/niobium nitride	1.6	68	28	2.43	0.5 M $KHCO_3$	0.9 V vs RHE	Ref. S25
$Au@Co_3O_4$	33	48	52	0.92	0.1 M $KHCO_3$	2.0 V vs SCE	Ref. S26
Fe-NC	2	60	40	1.50	0.1 M $KHCO_3$	0.6 V vs RHE	Ref. S27
Zn/Ni	8.5	50	40	1.25	0.1 M KCl	0.9 V vs RHE	Ref. S28
ZnO-CNT	0.2	25	75	0.33	0.1 M $KHCO_3$	0.9 V vs RHE	Ref. S29
Ag/TiO_2	110	80	20	4.00	0.1 M KOH	0.6 V vs RHE	Ref. S30

Reference

S2. T. Yamamoto, D. A. Tryk, A. Fujishima and H. Ohata, *Electrochimica Acta*, 2002, **47**, 3327-3334.

S3. C. Delacourt, P. L. Eidgway, H. B. Kerr, J. Newman, *J. Electrochem. Soc*., 2008, **155**, B42.

S4. J. J. Walch, G. Neri, C. L. Smith and A. J. Cowan, *Chem. Commun*., 2014, **50**, 12698-12701.

S5. P. Kang, Z. Chem, A Nayak, S. Zhang and T. J. Meyer, *Energy. Environ. Sci.* 2014, **7**, 4007-4012.

S6. A. S. Varela, N. R. Sahraie, J. Steinberg, W. Ju, H.-S. Oh and P. Strasser, *Angew. Chem. Int. Ed.,* 2015, **54**, 10758-10762.

S7. M. R. Singh, Y. Kwon, Y. Lum, J. W. Ager, III, and A. T. Bell, *J. Am. Chem. Soc.*, 2016, **138**, 13006-13012.

S8. Y. C. Li, D. Zhou, Z. Yan, R. H. Gonçalves, D. A. Salvatore, C. P. Berlinguette and T. E. Mallouk, *ACS Energy Lett*., 2016, **1**, 1149-1153.

S9. Q. Li, J. Fu, W. Zhu, Z. Chen, B. Shen, L. Wu, Z. Xi, T. Wang, G. Lu, J.-j. Zhu and S. Sun, *J. Am. Chem. Soc.*, 2017, **139**, 4290-4293.

S10. W. Sheng, S. Kattel, S. Yao, B. Yan, Z. Liang, C. J. Hawxhurst, Q. Wu and J. G. Chen, *Energy Env. Sci.*, 2017, **10**, 1180-1185.

S11. M. B. Ross, C. T. Dinh, Y. Li, D. Kim, P. D. Luna, E. H. Sargent and P. Yang, *J. Am. Chem. Soc.*, 2017, 139, 9359-9363.

S12. Z. B. Hoffman, T. S. Gray, K. B. Moraveck, T. B. Gunnoe, G. Zangari, *ACS Catal.,* 2017, **7**, 5381-5390.

S13. S. Guo, S. Zhao, X. Wu, H. Li, Y. Zhou, C. Zhu, N. Yang, X. Jiang, J. Gao, L. Bai, Y. Liu, Y. Lifshitz, S.-T. Lee and Z. Kang, *Nat. Commun*., 2018, **8**, 1038/1-9.

S14. F. M. Mota, D. L. T. Nguyen, J.-E. Lee, H. Piao, J.-H. Choy, Y. J. Hwang and D. H. Kim, *ACS Catal.*, 2018, **8**, 4364-4374.

S15. B. Qin, Y. Li, H. Fu, H. Wang, S. Chen, Z. Liu and F. Peng, *ACS Appl. Mater. Interfaces,* 2018, **10**, 20530-20539.

S16. H. Kim, H. Lee, T. Lim and S. H. Ahn, *J. Ind. Engin. Chem.,* 2018, **66**, 248.

S17. H. Li, P. Wen, D. S. Itanze, Z. D. Hood, X. Ma, M. Kim, S. Adhikari, C. Lu, C. Dun, M. Chi, Y. Qiu and S. M. Geyer, *Nat. Commun.*, 2019, **10**, 5724/1-10.

S18. M. Tomisaki, S. Kasahara, K. Natsui, N. Ikemiya and Y. Einaga, *J. Am. Chem. Soc.*, 2019, **141**, 7414-7420.

S19. N. Meng, C. Liu, Y. Liu, Y. Yu and B. Zhang, *Angew. Chem. Int. Ed.*, 2019, **58**, 18908-18912.

S20. R. He, X. Yuan, P. Shao, T. Duan and W. Zhu, *Small*, 2019, **15**, 1904882/1-7.

S21. A. S. Malkani, J. Anibal and B. Xu, *ACS Catal.*, 2020, **10**, 14871-14876.

S22. R. Daiyan, R. Chen. P. Kumar, N. M. Bedford, J. Qu, J. M. Cairney, X. Lu and R. Amal, *ACS Appl. Mater. Interfaces*, 2020, *12*, 9307-9315.

S23. B. Qin, Q. Zhang, Y.-H. Li, G. Yang and F. Peng, *ACS Appl. Mater. Interfaces*, 2020, **12**, 30466-30473.

S24. Q. He, D. Liu, J. H. Lee, Y. Liu, Z. Xie, S. Hwang, S. Kattel, L. Song and J. G. Chen, *Angew. Chem. Int. Ed.*, 2020, **59**, 3033-3037.

S25. Y. Liu, D. Tian, A. N. Biswas, Z. Xie, S. Hwang, J. H. Lee, H. Meng and J. G. Chen, *Angew. Chem. Int. Ed.*, 2020, **59**, 11345-11348.

S26. S.-Y. Zhang, J.-J. Ma, H.-L. Zhu and Y.-Q. Zheng, *New. J. Chem.*, 2020, **44**, 11808-11816.

S27. J. Zhao, J. Deng, J. Han, S. Imhanria, K. Chen and W. Wankg, *Chem. Engin. J.,* 2020, 389, 124323/1-7.

S28. M. Beheshti, S. Kakooei, M. C. Ismail and S. Shahrestani, Electrochimica Acta, 2020, 341, 135976/1-8.

S29. I. Hjorth, Y. Wang, Y. Li, M. E. M. Buan, M. Nord, M. Rønning, J. Yang and D. Chen, Catal. Today, DOI: https://doi.org/10.1016/j.cattod.2020.03.055.

S30. Y. E. Kim, B. Kim, W. Lee, Y. N. Ko, M. H. Youn, S. K. Jeong, K. T. Park and J. Oh, *Chem. Engin. J.,* DOI: https://doi.org/10.1016/j.cej.2020.127448

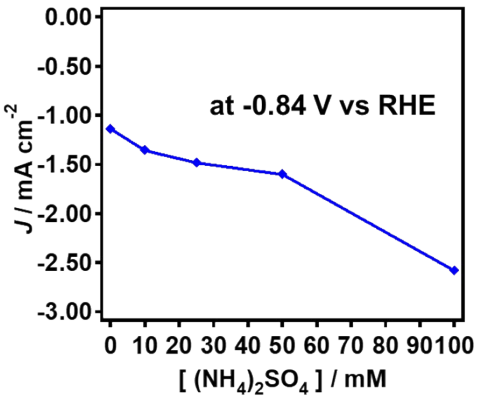

Fig. S1. Relation between the current densities at E = -0.84 V vs. RHE in 0.1 M Na_2SO_4–0.1 M $NaHCO_3$ containing various concentrations of $(NH_4)_2SO_4$.

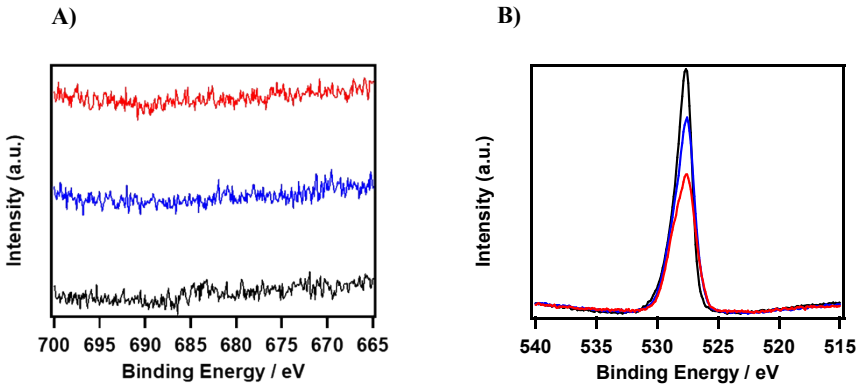

Fig. S2. F1s- and O1s-XP spectra of FTO electrodes before (black), after 30-min electrolysis in 0.1 M Na_2SO_4–0.1 M $NaHCO_3$ aq. (blue), and after 30-min electrolysis in 0.1 M Na_2SO_4–0.1 M $NaHCO_3$–0.1 M $(NH_4)_2SO_4$ aq. (red).

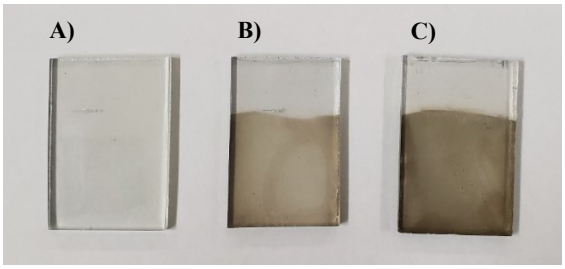

Fig. S3. Pictures of FTO electrodes before (A), after 30-min electrolysis in 0.1 M Na_2SO_4–0.1 M $NaHCO_3$ aq. (B), and after 30-min electrolysis in 0.1 M Na_2SO_4–0.1 M $NaHCO_3$–0.1 M $(NH_4)_2SO_4$ aq. (C).

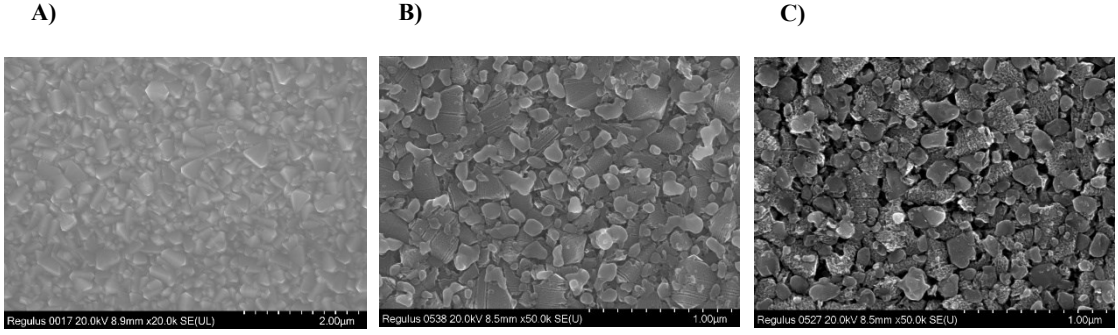

Fig. S4. SEM image of the surface of FTO electrodes before (A), after 30-min electrolysis in 0.1 M Na_2SO_4–0.1 M $NaHCO_3$ aq. (B), and after 30-min electrolysis in 0.1 M Na_2SO_4–0.1 M $NaHCO_3$–0.1 M $(NH_4)_2SO_4$ aq. (C).

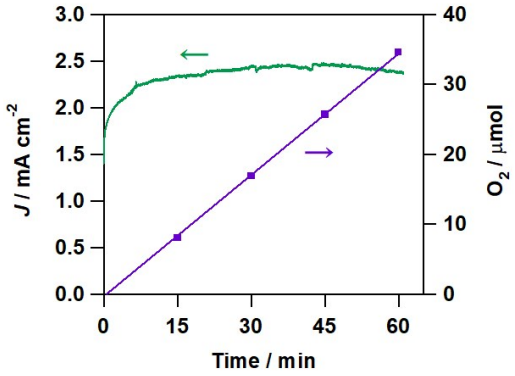

Fig. S5. Chronoamperometry curve and time evolution of O_2 at the GC anode in a three-electrode cell with the structure of GC | 0.1 M $(NH_4)HCO_3$ aq. (pH 6.7) | Nafion | 0.1 M $(NH_4)HCO_3$ aq. (pH 6.7) | FTO, Ag/AgCl under CO_2 flow with a constant rate of 100 mL min^{-1}. The potential of FTO electrode was maintained at -1.3 V vs. SHE.

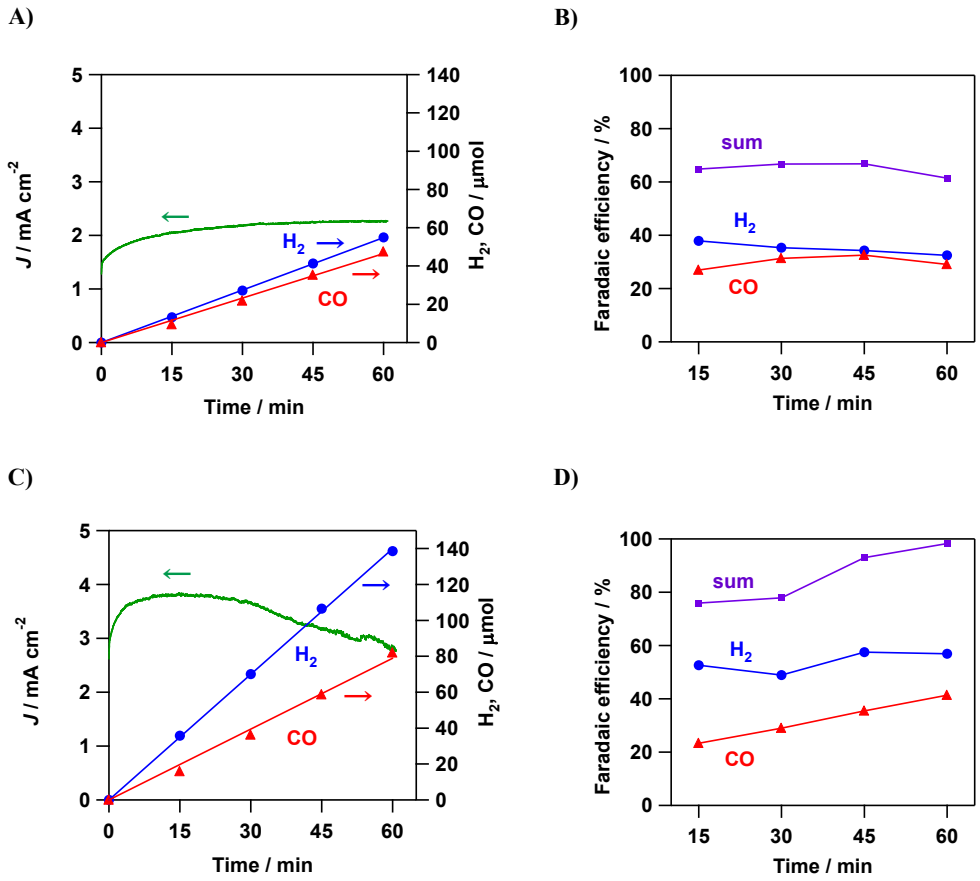

Fig. S6. (A) Chronoamperometry curves and time evolution of gaseous products in a three-electrode cell with the structure of GC | 0.1 M $NaHCO_3$ + 0.1 M Na_2SO_4 aq. (pH 6.9) | Nafion | 0.1 M $NaHCO_3$ + 0.1 M Na_2SO_4 aq. (pH 6.9) | FTO, Ag/AgCl under CO_2 flow with a constant rate of 100 mL min^{-1}. The potential of FTO electrode was maintained at -0.9 V vs. RHE. Each pH is the value at the initial state. (B) Faradaic efficiency of CO and H_2 generation under the same conditions. (C) Chronoamperometry curves and time evolution of gaseous products in a three-electrode cell with the structure of GC | 0.1 M $NaHCO_3$ + 0.1 M $(NH_4)_2SO_4$ aq. (pH 6.9) | Nafion | 0.1 M $NaHCO_3$ + 0.1 M $(NH_4)_2SO_4$ aq. (pH 6.9) | FTO, Ag/AgCl under CO_2 flow with a constant rate of 100 mL min^{-1}. The potential of FTO electrode was maintained at -0.9 V vs. RHE. (D) Faradaic efficiency of CO and H_2 generation under the same conditions.

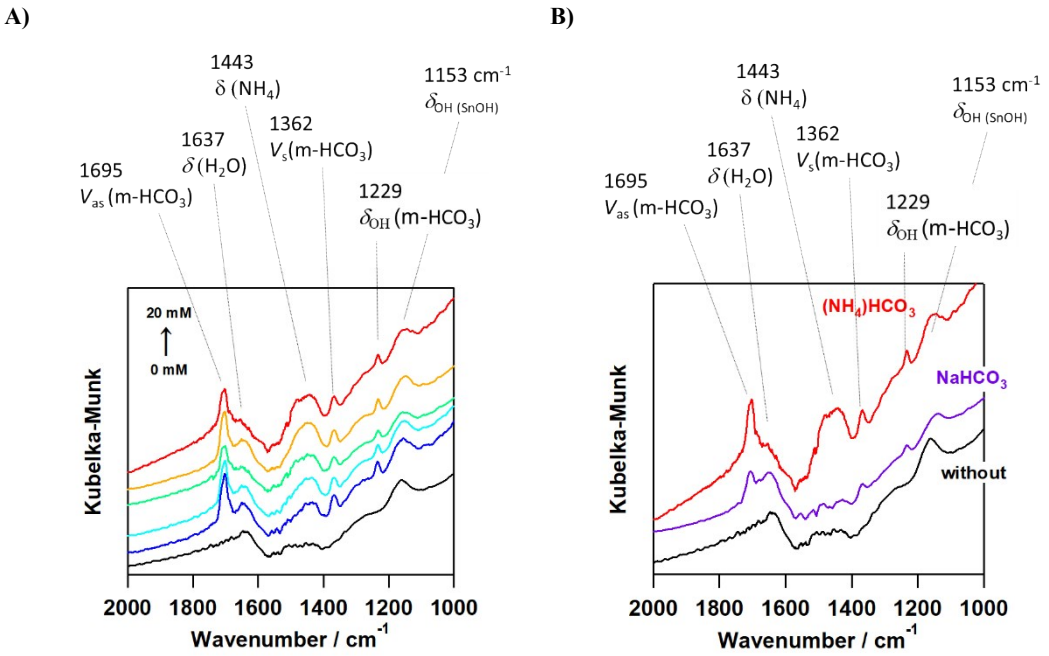

Fig. S7. (A) DRIFT spectra for NH_4^+ ion-adsorbed FTO particles from $(NH_4)HCO_3$ aqueous solutions with varying concentrations. (B) DRIFT spectra of HCO_3^- ion-adsorbed FTO particles from 20 mM $(NH_4)HCO_3$ and 20 mM $NaHCO_3$ aqueous solutions.